Available online at www.sciencedirect.com
SCIENCE DIRECT
Polymer 46 (2005) 9113–9125
polymer
www.elsevier.com/locate/polymer

Liquid crystalline elastomers based on diglycidyl terminated rigid monomers and aliphatic acids. Part 2. Mechanical characterization

Marta Giamberini[a,*], Pierfrancesco Cerruti[b], Veronica Ambrogi[b], Cosimo Vestito[b], Francesco Covino[b], Cosimo Carfagna[b,c]

[a]*Istituto per i Materiali Compositi e Biomedici, Consiglio Nazionale delle Ricerche, Piazzale Tecchio 80, 80125 Napoli, Italy*
[b]*Dipartimento di Ingegneria dei Materiali e della Produzione, Università di Napoli 'Federico II', Piazzale Tecchio 80, 80125 Napoli, Italy*
[c]*Istituto di Chimica e Tecnologia dei Polimeri ICTP-CNR, Via Campi Flegrei 34, 80078 Pozzuoli (Na), Italy*

Received 2 December 2004; received in revised form 18 March 2005; accepted 1 April 2005
Available online 29 August 2005

Abstract

In this paper the orientational behaviour and the mechanical properties of four LC elastomers, obtained by reacting two mesogenic epoxy monomers, DOMS and PHBHQ, with two aliphatic acids having four (AA) and eight (SA) methylene groups, respectively, have been studied.

Stress-relaxation experiments performed at a strain value $\varepsilon = 0.2$ showed shorter relaxation times and lower relaxation moduli for AA-based elastomers as compared with the PHBHQ-SA system.

Stress–strain curves of the LC elastomers showed the plateau attributed to the soft elasticity. The lower crosslink density in the case of DOMS-based elastomers affected the tensile properties adversely. Moreover, PHBHQ-SA was found to show poor strain recovery and it recovered the original size only upon heating to isotropic phase. This evidence was also confirmed by isostrain measurements.

Dynamic mechanical thermal analysis (DMTA) confirmed the existence of a heterogeneous, more branched structure in the case of DOMS-based systems. The particular features of the DMTA response strongly depend on the material composition and, in general, were found in agreement with other evidences from the literature.

Keywords: Liquid crystalline elastomers (LCE); Mechanical properties; Orientation

1. Introduction

Liquid crystalline elastomers (LCEs) are lightly crosslinked networks, in which rigid-rod LC molecules are incorporated into the polymer backbone, or linked to it via a flexible spacer. In the former case, they are called 'main-chain LCE', while in the latter they are known as 'side-chain LCE'. LCEs typically have low glass transition temperatures, low moduli and exhibit LC phase transitions due to the high mobility of the network strands. The combination of the entropic elasticity of polymer networks with the orientational ordering of anisotropic LC molecules is a fascinating concept, which has suggested new applications in chemistry, physics, material science, as well as new theoretical aspects [1,2]. Such systems have indeed shown spontaneous shape change at the phase transitions, strain-induced orientational transitions leading to new organized morphologies, peculiar dynamic-mechanical properties and soft elasticity [3–6]. Interest in such materials arises from their potential applications in the field of mechanical actuators (artificial muscles), optics and coatings of materials which can efficiently dissipate mechanical energy for, e.g. automotive and aerospace industry.

In Part 1 of this work we have reported the synthesis and characterization of two groups of LCEs obtained by reacting rigid-rod epoxy terminated molecules, namely *p*-bis(2,3-epoxypropoxy)-α-methylstilbene (DOMS) and 4′-(2,3-epoxypropoxy)phenyl-4-(2,3-epoxypropoxy)benzoate (PHBHQ), with aliphatic acids of general formula HOOC–$(CH_2)_n$–COOH, with *n* comprised between 4 and 8 [7]. The

* Corresponding author. Address: Departament de Química Analítica i Química Orgànica, Facultat de Química, Campus Sescelades, C/Marcel.lí Domingo, s/n-43007 Tarragona, Spain.
E-mail address: marta.giamberini@urv.net (M. Giamberini).

0032-3861/$ - see front matter © 2005 Elsevier Ltd. All rights reserved.
doi:10.1016/j.polymer.2005.04.093

curing reactions were investigated by DSC, FT-IR, rheological experiments, MALDI-TOF, NMR, and we found that, in the case of DOMS, the systems grow with a high degree of branching, giving rise to smectic A elastomers. In the case of PHBHQ, nematic elastomers resulted for acids with $n=4, 5$, and smectic A elastomers for higher values of n. We found that the aliphatic portion has a considerable effect on the mesophase stabilization. Finally, we put into evidence that all the LCEs under investigation exhibited the polydomain-to-monodomain transition upon stretching.

In this paper, our attention was focused in particular on four systems, namely PHBHQ-AA and DOMS-AA ($n=4$), PHBHQ-SA and DOMS-SA ($n=8$). The orientational and mechanical response to uniaxial stress was investigated as a function of time and temperature. This study was carried out bearing in mind that the state of order of these systems is not irreversibly fixed by covalent linkages, and that their glass transition temperatures are very close to room temperature. This implies that the behaviour of these materials is strongly affected by both the slow dynamics of relaxation and the gap between their T_g and the test temperature. As a consequence, the experiments were performed on samples lying in non-equilibrium conditions.

We performed stress–strain experiments on the LC elastomers. Stress relaxation behaviour at a relatively low strain value was also investigated. Isostrain tests on previously oriented samples were carried out to test their potentialities as mechanical actuators. Finally, we reported the preliminary results of dynamic mechanical thermal experiments.

2. Experimental

2.1. Materials

The mesogenic monomers *p*-bis(2,3-epoxypropoxy)-α-methylstilbene (DOMS) and 4′-(2,3-epoxypropoxy)phenyl-4-(2,3-epoxypropoxy)benzoate (PHBHQ) were synthesized according to the procedure described in a previous paper [8]. Elastomers were synthesized from epoxy monomers PHBHQ and DOMS by reaction with carboxylic acids of general formula HOOC–$(CH_2)_n$–COOH, with n comprised between 4 and 8, as it has been described in Part 1 [7]. In this paper, we have investigated on the mechanical properties of the systems obtained by reacting DOMS and PHBHQ with adipic acid (AA) and decanedioic acid (SA), respectively (DOMS-AA, PHBHQ-AA, DOMS-SA and PHBHQ-SA systems), whose thermal properties and mesophases are reported in Table 1.

Table 1
Thermal properties and mesophases of the systems under investigation

System	T_g (°C)	T_i (°C)	Mesophase
DOMS-AA[a]	33	67	S_A
DOMS-SA[a]	30	80	S_A
PHBHQ-AA[a]	37	61	N
PHBHQ-SA[a]	36	87	S_A

N and S_A stand for nematic and smectic A, respectively.
[a] Data from Ref. [7].

2.2. Characterization

2.2.1. X-ray diffraction

X-ray diffraction patterns were recorded by the photographic method using a Rigaku mod. III/D max generator, with a Ni-filtered Cu K_α radiation, at room temperature.

X-ray investigations were performed on LC elastomers stretched at $T>T_g$ up to different values of the strain $\Delta L/L_0$ (deformation rate = 50 mm/min), and subsequently quenched to the glassy state.

The dependence of the order parameter S on strain ($\Delta L/L_0$) was determined.

The value of S was calculated by elaborating the pattern generated by the oriented samples by means of Eqs. (1)–(3):

$$S = \tfrac{1}{2}(3\langle\cos^2\theta\rangle - 1) \tag{1}$$

$$\langle\cos^2 x\rangle = \frac{\int_0^{\pi/2} I(\cos^2 x)(\operatorname{sen} x)\mathrm{d}x}{\int_0^{\pi/2} I(\operatorname{sen} x)\mathrm{d}x} \tag{2}$$

$$\langle\cos^2\theta\rangle = 1 - 2\langle\cos^2 x\rangle \tag{3}$$

where x is the coordinate of an azimuthal scan performed on the diffraction pattern.

2.2.2. Dynamometric experiments

Dynamometric tests were performed on dumb-bell shaped specimens obtained according to ASTM D1708 standard test method. Experiments were carried out using a dynamometer INSTRON mod. 4204 mechanical testing machine, employing a 1 KN load cell. Temperature was controlled with a forced air chamber. Stress–strain tests were performed according to ASTM D412, at a crosshead displacement rate 50 mm/min. Testing temperatures were 40 °C for LC elastomers and 65 °C for samples after LC-to-isotropic transition.

Strain recovery of the elastomeric samples in the LC phase was measured at $T=45$ °C, by loading PHBHQ-SA and PHBHQ-AA up to 300 and 200% nominal strain, respectively. A crosshead displacement rate of 2.5 mm/min was chosen, and recovery was measured by loading the sample in the reversed strain direction.

2.2.3. Stress relaxation experiments

Stress relaxation experiments were performed on PHBHQ-AA, PHBHQ-SA and DOMS-AA at $T=40$ °C in uniaxial tension with the same experimental apparatus

described in Section 2.2.2 for dynamometric tests. Samples were extended up to initial strain $\varepsilon_0=0.20$, then the crosshead was stopped in order to keep the strain constant, and the force decay was measured as a function of time. The force was subsequently converted into nominal stress. The time was normalized by setting to zero the point at which crosshead was stopped.

The stress relaxation curves were fitted to a single exponential function as described by a modification of the Kohlrausch–Williams–Watt (KWW) equation [9], analogously to the analysis performed by Ortiz et al. [10] on stress relaxation data of DOMS-SA:

$$\sigma_n(t) = (\sigma_{\max} - \sigma_{\min})\exp(-t/\tau)^{\beta} + \sigma_{\min} \quad (4)$$

where t is the experimental time, $\sigma_{\max}$ is the instantaneous (unrelaxed) nominal stress at $t=0$, $\sigma_{\min}$ is the long-time (relaxed) stress at $t=\infty$ and τ is the characteristic relaxation time. The parameter β is a measure of the narrowness of the distribution.

The time-dependent relaxation modulus E_R, and the corresponding form of the KWW equation are given as follows:

$$E_R(t) = \frac{\sigma_n(t)}{\varepsilon_0} \quad (5)$$

$$E_R(t) = (E_0 - E_f)\exp(-t/\tau)^{\beta} + E_f \quad (6)$$

where $E_0=E_R$ is the instantaneous (unrelaxed) modulus, $E_f=E_R(t=t_f)\approx E_R(t=\infty)$ is the long-time (relaxed) modulus and t_f is the final time recorded in the stress relaxation experiment.

The relaxation strength is defined according to the equation:

$$\Delta = \frac{E_0 - E_f}{E_f} \quad (7)$$

β and τ were estimated from experimental data by rearranging Eq. (6) to:

$$\ln\ln[1/R(t)] = \beta\ln(t/\tau) \quad (8)$$

where $R(t)$ is equal to $(E(t)-E_f)/(E_0-E_f)$. In this form, a plot of the left-hand side of Eq. (8) versus the $\ln(t)$ gives a line whose slope is β and y-intercept is equal to $-\beta\ln\tau$.

2.2.4. Isostrain tests

Isostrain experiments were performed on a TA Instrument DMA 2980 with film/fibre tension clamps. Measurements were done on oriented DOMS-SA and PHBHQ-SA by heating through the LC-to-isotropic transition at 1 °C/min heating rate with the films under a small preload stress of about 0.1 KPa and a 2% isostrain. Samples were previously oriented in the rubbery state by uniaxial stress, up to a strain corresponding to a value of the order parameter $S=0.6$, and then quenched to the glassy state in order to retain the achieved orientation. The preload stress was parallel to the mesogen orientation direction. The dimensions of oriented samples were about $11\times9\times0.9$ mm^3 (length×width×thickness). They varied from sample to sample and were measured by a micrometer individually. Before heating, samples were allowed to equilibrate for 3 min at the initial temperature.

2.2.5. Dynamic mechanical thermal analysis (DMTA)

Dynamic mechanical thermal experiments were performed on polydomain samples by means of TA Instrument 2980 dynamic mechanical analyzer in the shear sandwich configuration, in the fixed frequency mode at frequencies of 0.1, 1, 10, 100 Hz, respectively. Surface areas of samples were about 80 mm^2 and their thickness was typically 1 mm, but slightly varied from sample to sample and was measured by a micrometer individually for each sample. The amplitude of the applied deformation was 5 μm, making the sample shear strain ε approximately 0.5%. Samples were annealed 1 h in the isotropic phase and were then slowly cooled down to room temperature before being analysed. DMTA experiments were performed by heating samples from room temperature to the isotropic phase at a rate of 1 °C/min; samples were previously equilibrated 15 min at the starting temperature.

3. Results and discussion

3.1. Orientational behaviour and calculus of the order parameter S

In order to clarify the orientational behaviour and to determine the dependence of the state of order (order parameter S) on strain ($\Delta L/L_0$), X-ray experiments were performed on crosslinked samples, on which an uniaxial mechanical stress was applied in the rubbery state. This stress was able to highly orient the networks. This phenomenon is a well-known characteristic of both main-chain and side-chain LCEs: when deformed in tension, the LC domains elongate and rotate their local director along the tensile axis to form a 'liquid single crystal' [10,11]. Depending on the material and on the external conditions, one can obtain samples of nematic or smectic phases that are without preferred orientation ('polydomains'), samples with moderate preferred orientation, or samples with high preferred orientation ('monodomains'). All the cured samples were stretched at $T>T_g$ up to different values of the strain $\Delta L/L_0$, and then quenched to the glassy state. The samples underwent a polydomain-to-monodomain transition and they became transparent as a consequence of the strain. As an example, the X-ray patterns of PHBHQ-SA, taken at room temperature, are shown at two different strain values ($\Delta L/L_0=0$ and $\Delta L/L_0=3.0$, respectively) (Fig. 1).

The X-ray pattern showed, for $\Delta L/L_0=0$ (Fig. 1(a)), a diffuse wide-angle halo indicating a disordered arrangement

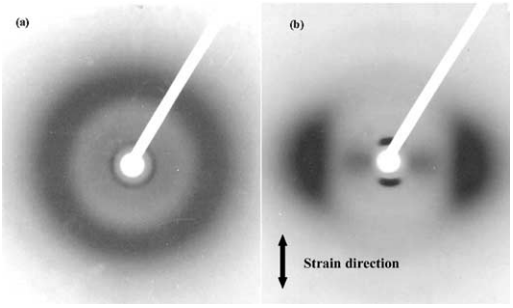

Fig. 1. Wide-angle X-ray pattern of PHBHQ-SA at: (a) $\Delta L/L_0=0$ and (b) $\Delta L/L_0=3$. The arrow indicates the stretching direction.

of mesogenic units. From the diameter of the outer maxima, calculations of the average intermolecular distance, D, i.e. the average distance between the long axes of adjacent molecules, can be done [7]. The inner diffraction ring is indicative of a smectic phase. In smectic phases, a stack of identical flat layers, parallel to each other, can be identified. In such phases, the inner maxima are related to the spacing of the smectic layers, d [7]. At this point the sample is opaque, indicating the existence of a 'polydomain' microstructure.

The X-ray pattern of the sample stretched ($\Delta L/L_0=3.0$) in the rubbery state and subsequently quenched to the glassy state is reported in Fig. 1(b). A broadened wide-angle reflection at the equator is visible, while the smectic layer reflections can be observed at the meridian, indicating a perpendicular orientation of the smectic layers to the stress direction [12]. From the inner diffraction maxima, the spacings of the smectic layers, d, could be calculated: the same values were obtained for oriented and unstrained samples within the experimental error. The sharpness of outer maxima gives information on the orientation of the LC director: a sharp maximum indicates an ordered packing and a broad maximum indicates disordered packing [12]. In particular, in the case of a monodomain, the intensity of the outer ring allows to calculate the orientational order parameter S, according to the Eqs. (1)–(3) reported in Section 2.2.1.

PHBHQ-SA, DOMS-SA, DOMS-AA and PHBHQ-AA samples were analysed (Table 1).

The first three systems exhibit a S_A phase, while the fourth is nematic. We performed the X-ray experiments on unstretched elastomers as well as on the same samples immediately after being stretched and subsequently quenched to the glassy state. In these conditions, the systems are in a non-equilibrium, 'unrelaxed' state. The value of the order parameter, S, in correspondence to different deformation values was calculated. Due to slow relaxation phenomena, S was expected to vary in a long time scale to a different extent, depending on the system under examination. Fig. 2 reports the value of S, calculated from the XRD patterns, versus elongation for the four systems.

PHBHQ-SA and DOMS-SA reach the same value of S (i.e. $S=0.75$) at about the same elongation value ($\Delta L/L_0=1.7$): that is, the instantaneous orientation seems to be independent of the nature of the rigid core in the elastomer. Differently, in the case of DOMS-AA, a slightly higher value of the order parameter ($S=0.8$) is reached in correspondence to $\Delta L/L_0=1.0$. This suggests that the network instantaneous orientation obtained by mechanical stretching occurs faster in the case of shorter aliphatic spacers. That is, for shorter alkyl chains, the overall imposed strain is directly involved in the orientation of the LC director. In the case of longer chains, it is likely that mechanical stretching is required for the uncoiling of the aliphatic portions as well. As for nematic PHBHQ-AA, a lower value of S is reached (i.e. $S=0.63$) at $\Delta L/L_0=1$.

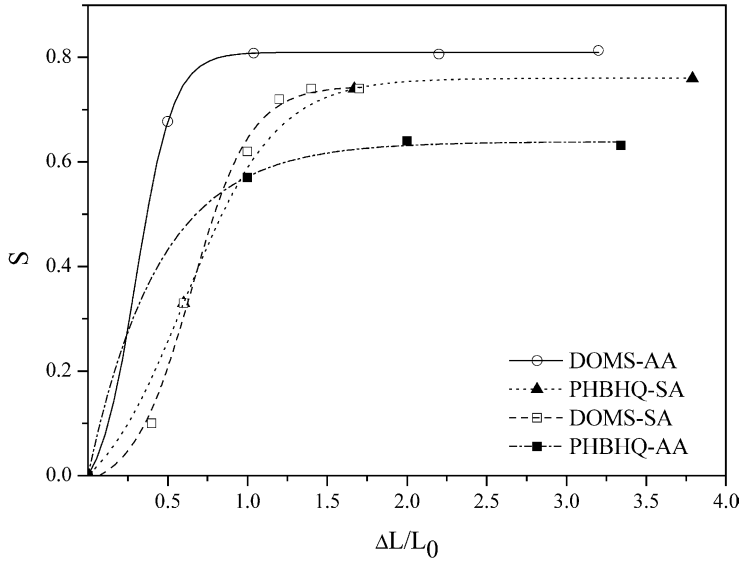

Fig. 2. Order parameter S versus strain $\Delta L/L_0$ for: (○) DOMS-AA; (□) DOMS-SA; (▲) PHBHQ-SA; (■) PHBHQ-AA.

Table 2
Mechanical properties under uniaxial tension of the elastomers under investigation

Sample (test temperature, °C)	E (MPa)	σ_{max} (MPa)	ε_{max} (mm/mm)
PHBHQ-SA (40)	29.3±0.4	12.2±0.4	3.1±0.1
PHBHQ-AA (40)	26.3±1.1	9.3±0.2	2.3±0.2
DOMS-AA (40)	15.0±4.4	4.5±0.9	1.2±0.2
DOMS-SA (45)[a]	16.5	7.5	2.8
PHBHQ-AA (65)	0.4±0.2	0.4±0.1	1.4±0.1

[a] Data from Ref. [16].

3.2. Stress–strain experiments

We have already pointed out in Section 3.1 that the polydomain structure undergoes the 'polydomain-to-monodomain (P–M)' transition [13] by applying external fields, in particular an uniaxial mechanical extension. The director alignment proceeds via the reorientation of correlated domains, while keeping their characteristic size approximately constant. A monodomain phase results, where the mesogenic units are preferentially aligned along a single reference direction represented by a unit vector [14]. The transition is accompanied by a very distinct stress–strain plateau, due to the soft-elastic response of rotating LC domains [15]. A typical stress–strain curve of an LC elastomer is thus characterized by the presence of three regions [16]: at small strains, the sample deforms in a linear manner, exhibiting a typical rubber modulus (turbid sample); at intermediate strains, a reversible P–M transition leads to a plateau in the stress–strain curve, due to the soft-elastic response [17]; at large strains, the modulus increases again and only a small amount of additional orientation is achieved (transparent sample). Recently, the elastic properties of main chain liquid crystalline elastomers, formed by crosslinking chains in a strongly nematic state, have been modelled, and it has been shown that hairpin defects can also play a crucial role in the occurring of a plateau in the stress–strain curve [18].

Table 2 reports the elastic modulus (E), ultimate tensile stress (σ) and strain (ε) obtained from stress–strain tests performed on elastomers at a temperature above glass transition. The stress–strain curves of LC samples are shown in Fig. 3.

The most striking evidence results in the lower ultimate strength and elongation to break exhibited by DOMS-containing elastomers in comparison with those containing PHBHQ.

Great attention should be paid in analysing the results of the stress–strain tests, as they strongly depend on the specific experimental conditions used. Two factors, the glass transition and the slow relaxation behaviour, strongly affect the stress–strain response of the elastomers under investigation, since the experimental temperature was very close to the T_g of the samples and such systems typically exhibit slow relaxation of stress [10,19].

However, one has to consider that $T_{test}-T_g$ values are very similar for all the analysed samples (Table 3). Furthermore, as evidenced by the stress relaxation results (Section 3.2) the decrease of modulus with the relaxation before the P–M transition appears to be significant for DOMS-AA and relatively small for PHBHQ-SA and PHBHQ-AA systems.

This entails that the differences in modulus values for the analysed systems would be even higher in a relaxed state. As a consequence, at least from a qualitative point of view, the different growth mechanism of the LC elastomers [7] can be assumed to affect the stress–strain behaviour.

In their studies, Flory and Yanko [20,21] found that the

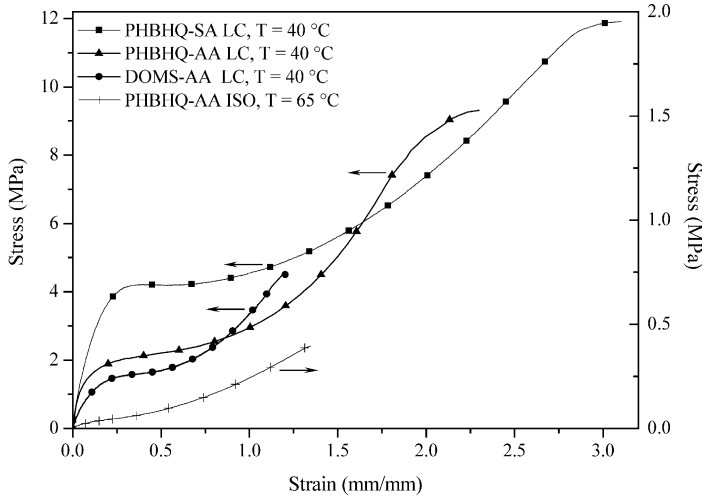

Fig. 3. Nominal stress versus nominal strain for: (■) PHBHQ-SA in the LC phase at $T=40$ °C; (▲) PHBHQ-AA in the LC phase at $T=40$ °C; (●) DOMS-AA in the LC phase at $T=40$ °C; (+) PHBHQ-AA in the isotropic phase at $T=65$ °C.

Table 3
Stress-relaxation parameters from uniaxial tension experiments at initial strain prior to the polydomain-to-monodomain transition

Sample	$T_{test}-T_g$ (°C)	Δ (MPa)	β	τ (s)	E_f (MPa)[a]
PHBHQ-AA	3	8.6	0.35±0.01	50±4	0.47
PHBHQ-SA	4	0.84	0.68±0.01	1274±27	6.0
DOMS-AA	7	3.3	0.40±0.01	118±7	2.6

[a] Error: ±1%.

tensile strength of crosslinked rubbers increased with number-average molecular weight of the starting uncrosslinked polymer, up to a limiting value. The elongation to break also increased with molecular weight. The effect of the initial molecular weight on the properties of vulcanized rubbers is a reflection of the change in crosslink density and an effect of fewer imperfections, such as dangling chain ends in the network, as molecular weight increases. In the first part of this work [7], MALDI-TOF experiments showed that DOMS-based systems, when compared to those containing PHBHQ, reached a lower molecular weight before the formation of an insoluble gel. In addition, the epoxy group conversion occurred in a minor extent in the case of DOMS. This was related to the significant occurrence of side reactions, responsible for the higher extent of branching in DOMS systems and anticipated gel-times, as shown by DSC and rheological experiments. NMR confirmed that DOMS-based systems undergo branching reaction during the growth of the pre-polymer chains. Higher branching extent results in a lower crosslink density and therefore in higher number of chain ends acting as imperfections in the structure, which could affect the strength properties adversely.

Fig. 3 also shows a comparison between the deformation behaviour of PHBHQ-AA in the nematic phase with that in the isotropic phase: it can be noticed that the phase nature also affects the stress–strain behaviour of elastomers significantly. Analogously to conventional elastomers, the stress–strain curve of the isotropic PHBHQ-AA does not show any plateau region. This also resulted from the comparison of stress–strain curves of DOMS-SA in the smectic and in the isotropic phase [16]. Moreover, a marked decay of mechanical properties was observed in the case of isotropic PHBHQ-AA with respect to the LC system. In this case, the effect of the temperature must be also taken into account. In fact, it has been shown that for crosslinked systems the rupture stress decreases steadily as the temperature increases [22]. Since the phase transition to isotropic PHBHQ-AA occurs at high temperature, the mutual contributions of temperature and nature of phase on tensile properties are not distinguishable.

PHBHQ-SA and PHBHQ-AA samples were loaded up to 300 and 200% nominal strain at a temperature above T_g, and then the strain direction was reversed to measure mechanical hysteresis (Fig. 4).

For a single cycle, the area of the loop cannot be equated to dissipated energy because the point of zero stress at the end of the cycle does not necessarily correspond to zero stored energy: after removal from the instrument, the sample can undergo some modification with further creep recovery [23].

The strain values were selected as the elongation to break point in the stress–strain curve (Fig. 3). As shown in Fig. 4, PHBHQ-SA exhibits 33% recovery upon unloading. At the end of the experiment, once it was removed from the grips, the sample retained its orientation and dimension, and recovered the original size only upon heating to isotropic phase. The recovery extent is lower than a conventional elastomer, but it is higher than that reported in literature for DOMS-SA [16]. In that paper, samples were loaded up to different elongations and the nominal strain recovery registered, after 290% nominal strain, was only 17%.

In the case of PHBHQ-AA, higher strain recovery was found. After orientation by uniaxial stress, the sample recovered 65% of the applied strain in the experimental conditions, when the stress was removed [24].

3.3. Stress relaxation experiments

Plots of the relaxation moduli versus time for PHBHQ-AA, PHBHQ-SA and DOMS-AA systems are shown in Fig. 5.

Table 3 reports the stress relaxation parameters, Δ, β and τ of the same systems calculated as reported in Section 2.2.3.

Samples were uniaxially stretched at 40 °C up to a strain

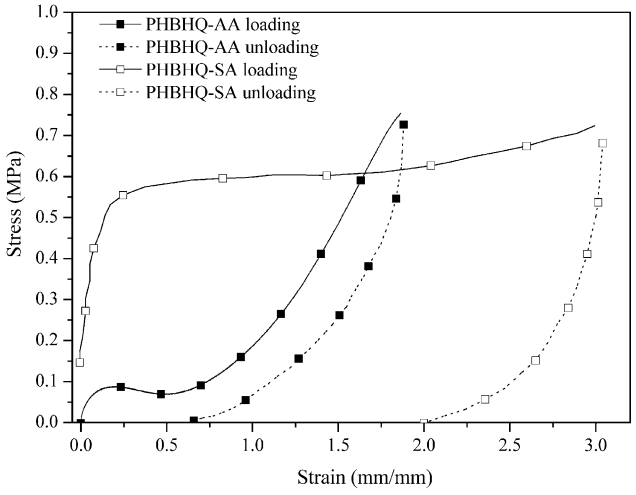

Fig. 4. Nominal stress versus nominal strain at $T=40$ °C for: (■) PHBHQ-AA and (□) PHBHQ-SA in uniaxial tension on loading and unloading.

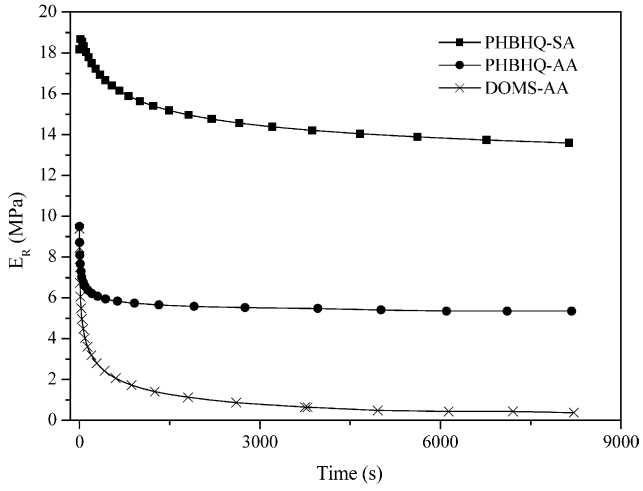

Fig. 5. Plot of the relaxation moduli versus time for the LCEs: (■) PHBHQ-SA, (●) PHBHQ-AA and (×) DOMS-AA.

$\varepsilon_0 = 0.20$, i.e. prior to the polydomain-to-monodomain transition, as inferred from the stress–strain experiments reported in Section 3.2. As soon as the strain reached the set value, the crosshead was stopped and the force decay was monitored as a function of time. The experiments were performed at a temperature very close to the T_g. This implies that the relaxation response may be also affected by the glass transition.

In their work, Ortiz et al. [10] found that, the strength of relaxation Δ, the parameter β and the relaxation time τ for DOMS-SA were approximately constant in the range of strain values between 0.15 and 2.61, i.e. before and after the polydomain-to-monodomain transition, while the final relaxation moduli were affected by the degree of macroscopic orientation. This suggested that the relaxation behaviour is different when polydomain or monodomain structures are considered. DOMS-SA surprisingly exhibited a large amount of stress relaxation ($\Delta = 2.33$), given its large mechanical hysteresis [16]: a possible explanation for this phenomenon, proposed in Ref. [10], is that the local smectic order is transiently disrupted during deformation and reorientation of the LC domains. The free energy penalty for this disruption could provide a driving force for reversion back to the original, undeformed state and therefore facilitate local chain relaxation.

From the time-dependent relaxation moduli plots reported in Fig. 5, it is observed that the three samples exhibit a similar behaviour, although higher values of modulus are associated to PHBHQ-SA. Table 3 shows that the system PHBHQ-AA exhibits a markedly higher value of Δ and a shorter characteristic relaxation time, τ, as compared with the other systems under investigation: the presence of the less-ordered nematic phase may be responsible for the different behaviour.

PHBHQ-SA was found to exhibit the lowest value of Δ, and the highest values of β and τ. This could be an effect of the network morphology. It has been shown that in an ideal rubber the stress remains constant at all times during a stress relaxation test [25]. However, in practice, crosslinked elastomers can have very imperfect structures that contain dangling chain ends and branched molecules only partly incorporated into the network. These structure defects lead to a decrease of stress relaxation moduli, as compared with systems characterized by more regular networks [25]. In Part 1 of this work we have reported that the occurrence of side reactions during the cure was responsible for the higher extent of branching in DOMS-based systems. This led to the formation of a very irregular network compared to systems based on PHBHQ. Therefore, low stress relaxation moduli would be expected for DOMS containing elastomers (Fig. 5).

3.4. Isostrain experiments

We have previously found that the systems obtained by reaction with AA, when oriented by uniaxial stress, rapidly recover the initial polydomain dimensions in the rubbery state, when the stress is removed: for these systems, the 'stress-induced' monodomain structure is clearly an extreme non-equilibrium situation. Therefore, isostrain measurements were carried out only on previously oriented PHBHQ-SA and DOMS-SA samples, by keeping a constant strain = 2% on the films along the stretching direction, and measuring the force generated as a function of the temperature, in analogy with experiments reported in the literature for side-chain nematic elastomers [5]. The development of retractive stress during the measurement is related to the entropy change [26,27]: the maximum retractive force in the film is developed when it is heated through the LC-I transition, as a consequence of the conformational change from oriented LC to isotropic random-coil [5]. The experiment stopped when the sample was broken as a result of the retractive force. However, it must be pointed out that, in our case, measurements are also affected by the relaxation behaviour: therefore, the force developed on heating cannot be, in any case, exclusively ascribed to the isotropization of the samples. The results of the isostrain tests are reported in Fig. 6.

Temperature is normalized with respect to the isotropization temperature of the unoriented samples, as inferred by DSC. The slope of the stress versus temperature curve is small in the smectic phase and, as expected, shows a sharp increase in correspondence to isotropization. In the case of DOMS-SA the onset of the retractive force lies at $T/T_i = 1.1$: this is not surprising, because it was reported that for this system the isotropization temperature is increased of about 10 °C, as a consequence of the orientation [28].

In the transition region, the slopes of the stress versus temperature plots were found to be 0.050 MPa/°C for PHBHQ-SA and 0.043 MPa/°C for DOMS-SA: these values are several orders of magnitude higher than typical values of vulcanized rubbers subjected to different isostrains [29].

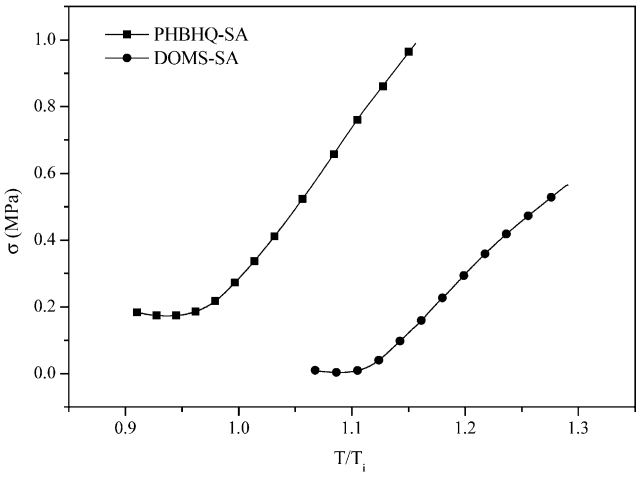

Fig. 6. Isostrain measurement at 2% strain on heating the samples through the LC to isotropic phase transition for: (■) PHBHQ-SA and (●) DOMS-SA.

3.5. Dynamic mechanical thermal analysis

Figs. 7–10 report the temperature dependence of the real part G' of the shear modulus (a) and of tan $\delta = G''/G'$ (b), at 0.1, 1, 10 and 100 Hz, for DOMS-AA, DOMS-SA, PHBHQ-AA, and PHBHQ-SA, respectively. Temperature is normalized with respect to the isotropization temperature, as determined by DSC second heating scan at a heating rate of 10 °C/min. The x-axis position of the glass transition temperature, determined by DSC, has been marked on the graphs.

In the plot of G' of DOMS-AA (Fig. 7(a)), higher frequencies result in higher values of modulus [30], which exhibits a sharp drop at the glass transition.

In correspondence to the smectic-to-isotropic transition, a step can be observed, which is more evident at higher frequencies, followed by a 70% reduction of G' within a temperature range of about 10 °C. This anomaly can be attributed to the disappearance of the lamellar structure, which is associated with the smectic A phase [31]. In a recent paper [32], Weilepp et al. give a qualitative explanation of the effect of the smectic A order on the shear modulus of a polydomain, side-chain liquid crystalline elastomer: the mesogens linked to one specific polymer backbone are generally supposed to belong to different smectic layers or even different smectic domains. So, different polymer backbones are connected through the mesogens, which are trapped in different smectic layers or domains, respectively. This gives rise to a network structure, which is in principle transient, where, however, steric hindrance and entanglements can prevent a complete relaxation of the applied stress. This implies a dramatic lifetime enhancement of the elastic modes in these systems and explains the reason for the observed step in the G' curve at the smectic A-to-isotropic transition. In principle, this explanation can be also applied to our smectic A systems.

After isotropization, for frequencies $\leq$10 Hz and for $T/T_i \geq 1.25$, DOMS-AA is in its hydrodynamic regime and G' increases with temperature (Fig. 7(a)), as predicted by the classical rubber elasticity theory [26].

A similar trend was also observed in the temperature dependence of G' for DOMS-SA (Fig. 8(a)).

In this case, two steps can be observed in the isotropization region. This could be explained by considering the growth mechanism of this system, which was discussed in the first part of this work: in fact, it was found that, in the case of DOMS, the reaction can proceed with higher degree of branching, and it probably gives rise to isolated, gelificated microdomains in its early stages. The final structure of the resulting network is therefore expected to be quite heterogeneous, and it could be characterized by a number of differently ordered regions, which exhibit a range of isotropization temperatures. The heterogeneous structure of DOMS-SA can be also inferred from the analysis of tan δ curve (Fig. 8(b)): in this case, in addition to the peaks which can be associated to the glass transition and to the isotropization, respectively, a number of shoulders are evident. This suggests the existence of portions of chain, with different local mobility. In the case of DOMS-AA, tan δ curve (Fig. 7(b)) exhibits two peaks, which tend to merge with increasing frequencies: the former is related to the glass transition, the latter to the isotropization. The contribution of second peak tends to prevail at the higher frequencies and finally becomes predominant with respect to the former one. No shoulders are evident throughout the range of stability of the LC phase. Nevertheless, the quite higher value of tan δ with respect to DOMS-SA, suggests the existence of nematic portions which tend to increase the sample mechanical loss, especially at higher frequencies. Clarke et al. [33] reported that the fluctuations in the nematic director lead to a significant increase in mechanical loss, giving rise to 'dynamic soft elasticity'; on the contrary, the smectic layers appear to increase mechanical rigidity and to reduce the internal dissipation. Fig. 9(a) reports G' versus reduced temperature for PHBHQ-AA system.

In the case of this nematic elastomer, only a small anomaly at the lowest frequency can be observed as the isotropization temperature is approached. At higher frequencies, no noteworthy effect can be put into evidence at the isotropization, and the considerable drop of G' can be ascribed to the transition from the glassy to the rubbery state. The hydrodynamic regime is reached only at the lowest frequency and in the isotropic phase, far from the isotropization temperature. Similar results have been recently reported for a polydomain, side-chain elastomer, which exhibits only nematic phase [34]. Dramatic effects have been theoretically predicted in the case of monodomain nematic elastomers sheared in certain geometries [35]. However, a previous investigation performed by Gallani et al. on a polydomain elastomer led to the conclusion that the response to an imposed oscillating shear is insensitive to the nematic-to-isotropic transition

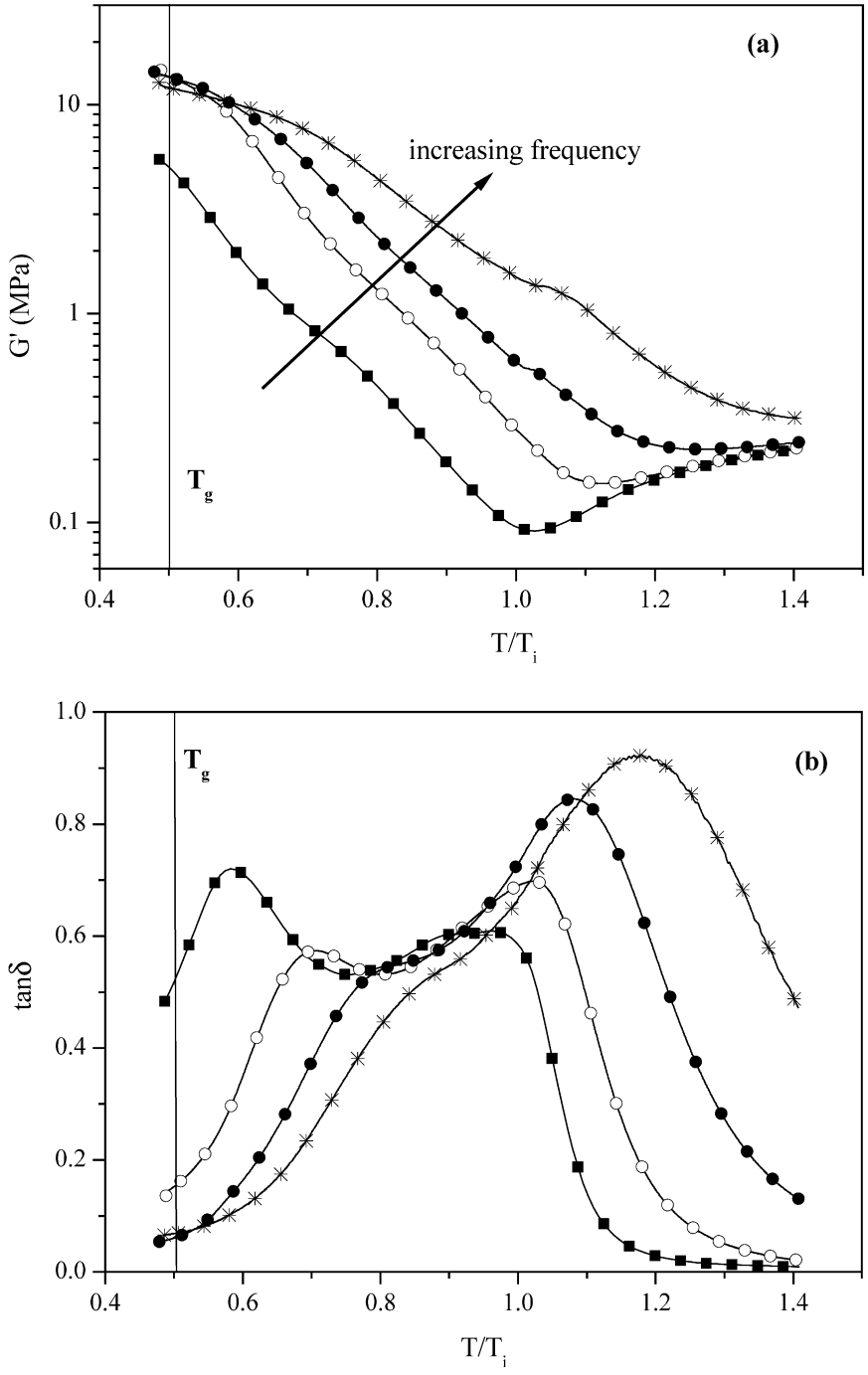

Fig. 7. Storage modulus G' (a) and loss factor tan δ (b) versus reduced temperature of unoriented DOMS-AA at (■) 0.1, (○) 1, (●) 10 and (*) 100 Hz isofrequency. The position of T_g as determined from DSC is indicated on the abscissa axis.

[36]. On the other hand, it was pointed out by other authors [37] that this result could depend either on the presence of smectic pre-transitional effects in the small nematic range of the elastomer under investigation, or on the fact that the effect in the nematic range could be masked by the glass transition. In the same paper [37], these authors examined the nematic-to-isotropic transition in the G' versus temperature curve for different monodomain, side-chain elastomers, and they found that this transition was much more diffuse in the case of an elastomer containing side-chain and main-chain nematic polymers in approximately equal proportion. In a more recent paper [38], the same authors reported that Master Curves could be built, between the glassy state and the nematic-to-isotropic transition, when this class of elastomers underwent shear in the geometry that allows the director rotation. Above $T_{n\rightarrow i}$, the modulus rises substantially, since the internal relaxation is no longer able to reduce the elastic response (i.e. soft

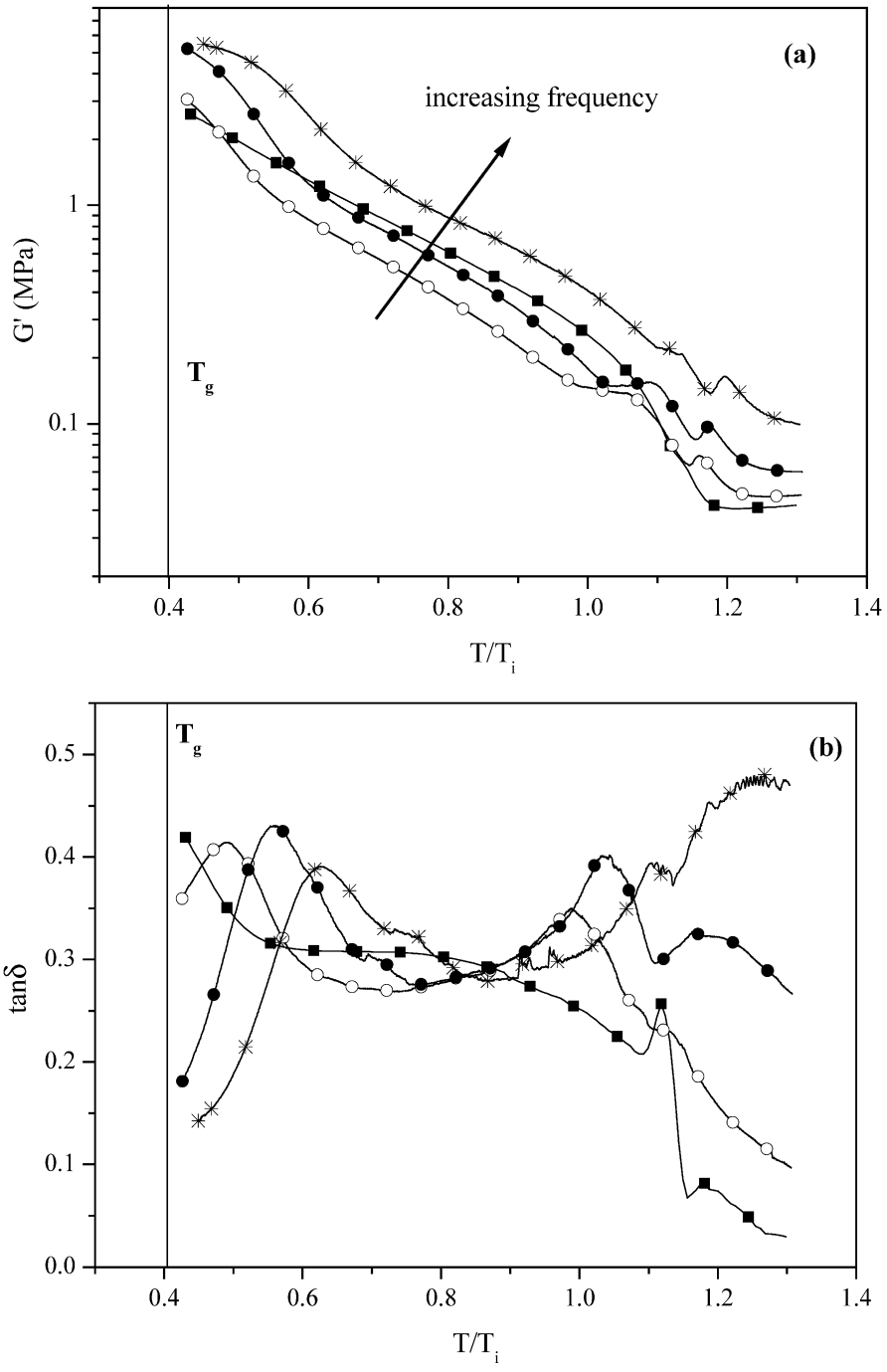

Fig. 8. Storage modulus G' (a) and loss factor tan δ (b) versus reduced temperature of unoriented DOMS-SA at (■) 0.1, (○) 1, (●) 10 and (*) 100 Hz isofrequency. The position of T_g as determined from DSC is indicated on the abscissa axis.

elasticity disappears) [38]. Therefore, the particular features of the response depend both on the material composition and on the nematic director texture and orientation, with respect to the applied strain. In a polydomain elastomer or in an overcrosslinked network, the required nematic director rotation may be prevented by internal constraints, and this could mask the soft elasticity.

Tan δ curve (Fig. 9(b)) exhibits a single broad peak with a considerable value of the loss factor, which is comprised between 0.8 and 1, approximately, in agreement with the presence of the nematic phase. The apparent discrepancy between the G' (where no noticeable effect attributable to soft elasticity was observed) and tan δ curves (whose feature can be instead ascribed to soft elasticity), is not surprising. In fact, in the case of a monodomain, nematic elastomer, containing side-chain and main-chain nematic polymers in approximately equal proportion [39], a unique set of time–temperature shift factors to simultaneously superpose G'

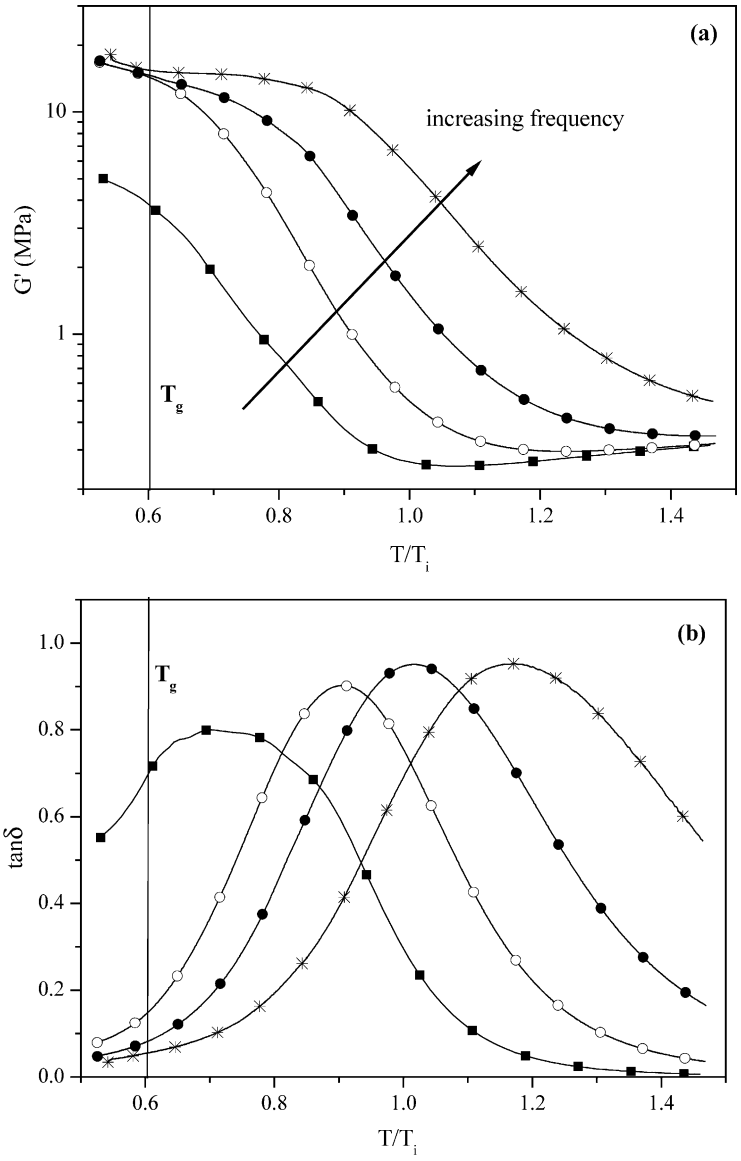

Fig. 9. Storage modulus G' (a) and loss factor tan δ (b) versus reduced temperature of unoriented PHBHQ-AA at (■) 0.1, (○) 1, (●) 10 and (*) 100 Hz isofrequency. The position of T_g as determined from DSC is indicated on the abscissa axis.

and G'' could not be found. The authors of that paper concluded that in this internally constrained system the relaxation of the elastic modulus is governed by different physical mechanisms, with respect to the dissipative processes.

When we examine the G' versus T/T_i curve for PHBHQ-SA (Fig. 10(a)), we can hardly notice a very small step in correspondence of the isotropization for frequencies ≥ 1 Hz.

The curve mainly shows the effects of the glass transition and, in our experimental conditions, the variations of G', arising from the smectic-to-isotropic transition, are probably masked by the more important consequences of this relaxation. The same conclusions can be deduced from tan δ curve (Fig. 10(b)): a very low and broad peak, which turns into a shoulder at higher frequencies, can be noticed in correspondence to the isotropization. The clearly evident phenomenon is the glass transition, which gives rise to a well-defined peak; the loss factor has generally low values at all the investigated frequencies, which is coherent with the presence of a smectic phase [33].

4. Conclusions

In this paper we have reported the orientational behaviour, the mechanical, and the dynamic–mechanical characterization of four LC elastomers, namely DOMS-AA, DOMS-SA, PHBHQ-SA and PHBHQ-AA, obtained by reacting two mesogenic epoxy monomers, DOMS and PHBHQ, with aliphatic acids having four (AA) or eight (SA) methylene groups, as described in Part 1. The first

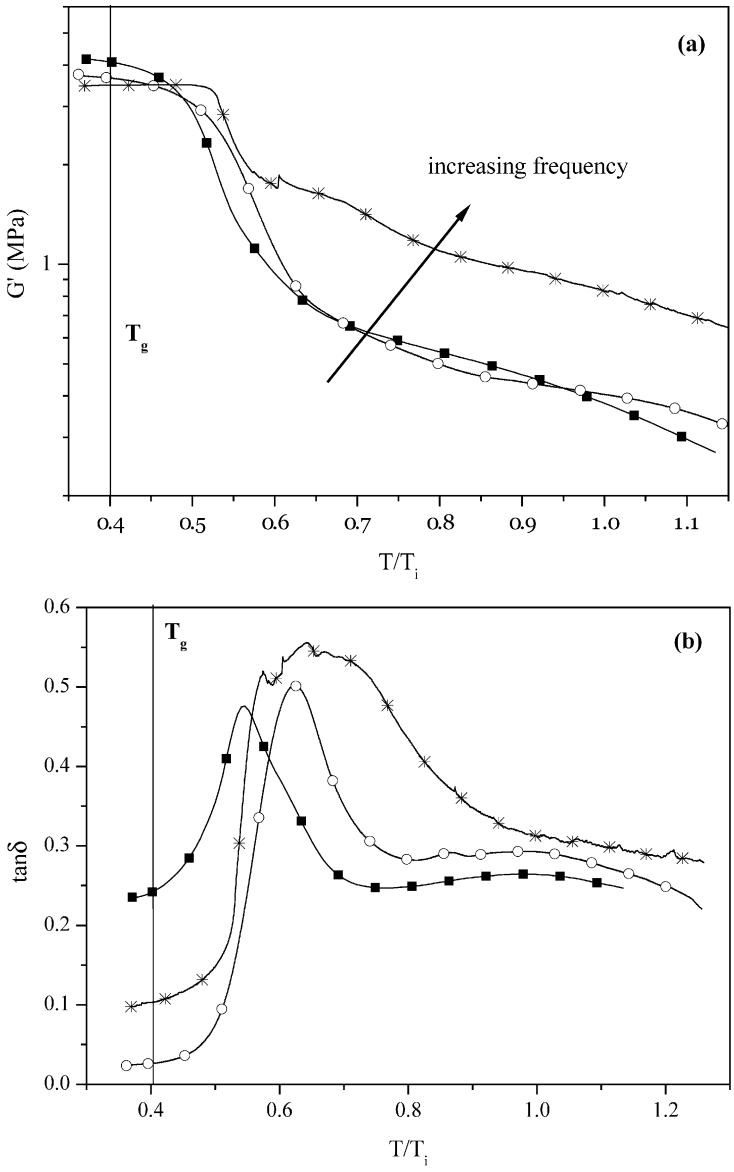

Fig. 10. Storage modulus G' (a) and loss factor tan δ (b) versus reduced temperature of unoriented PHBHQ-SA at (■) 0.1, (○) 1 and (*) 100 Hz isofrequency. The position of T_g as determined from DSC is indicated on the abscissa axis.

three elastomers exhibit a smectic A phase, while the last one is nematic.

X-ray diffraction experiments on stretched samples showed that all the samples can be oriented by uniaxial stress in the rubbery state, up to a value of the order parameter S ranging between 0.6 and 0.8, depending on the system under investigation.

Stress-relaxation experiments performed on polydomain samples showed a considerable relaxation in the case of PHBHQ-AA and DOMS-AA, while PHBHQ-SA exhibited a different behaviour, with a lower relaxation strength and a longer value of relaxation time.

In all cases, stress–strain curves of the LC elastomers showed the plateau attributed to the soft elasticity. PHBHQ-based systems showed superior mechanical properties than DOMS-based systems: this was attributed to a different mechanism of growth which, in the case of DOMS, gives rise to a lower crosslink density and thus to a higher number of chain ends acting as irregularities in the structure, which affect the tensile properties adversely.

It was found that SA-based systems exhibit poor strain recovery, i.e. they kept most of the orientation and dimensions when the strain direction is reversed, recovering the original size only upon heating to the isotropic phase. On the other hand, the AA-based systems tend to recover their polydomain morphology and dimensions as soon as they are heated above T_g.

Isostrain measurements were carried out on previously oriented SA-based samples by keeping a constant strain on the films along the stretching direction and measuring the force generated as a function of the temperature. These experiments showed that the oriented samples develop a

considerable retroactive stress when heated through the LC-I transition, as a consequence of their conformational change.

Dynamic mechanical thermal analysis (DMTA) was performed on the unoriented four elastomers. In the case of DOMS-based systems, the G' and tan δ curves showed the features already reported in the literature for other smectic systems, and also confirmed the existence of a heterogeneous, more branched structure. In the case of PHBHQ-SA, DMTA mainly showed the effects related to the glass transition and, under the experimental conditions used, the features arising from the smectic-to-isotropic transition were probably masked by the more important consequences of this relaxation. However, the loss factor was found to be generally low at all the investigated frequencies, which is coherent with the presence of a smectic phase. In the case of the nematic PHBHQ-AA, only a small anomaly in the storage modulus at the lowest frequency could be observed in proximity to the isotropization. At higher frequencies, no noteworthy effect could be put into evidence at the isotropization; differently, a considerable value of the loss factor was found, in agreement with the presence of the nematic phase.

However, it must be pointed out that most experiments were performed in non-equilibrium conditions, so that the behaviour of these materials is affected by the slow dynamics of relaxation. This implies that no definitive conclusions about the correlations between the structure of the systems and their behaviour could be established. Anyway, we consider these experiments as a first screening of the properties of the systems, in order to test their potentialities and to define future synthetic strategies.

Acknowledgements

The authors would like to thank Rodolfo Morra for his precious help in performing mechanical tests. Financial support of MIUR-COFIN 2003 project is gratefully acknowledged.

References

[1] Mayer S, Zentel R. Curr Opin Solid State Mater Sci 2002;6:545–51.
[2] Brand HR, Finkelmann H. Physical properties of liquid crystalline elastomers. In: Demus D, Goodby J, Gray J, Spiess HW, Vill V, editors. Handbook of liquid crystals. Weinheim: Wiley-VCH; 1998. p. 277.
[3] Warner M, Terentjev EM. Prog Polym Sci 1996;21:853–91.
[4] Stannarius R, Köhler R, Dietrich U, Tolksdorf C, Zentel R. Phys Rev E 2002;65:41707.
[5] Thomsen III DL, Keller P, Naciri J, Pink R, Jeon H, Shenoy D, et al. Macromolecules 2001;34:5868–75.
[6] Wermter H, Finkelmann H. e-Polymers 2001;013.
[7] Ambrogi V, Giamberini M, Cerruti P, Pucci P, Menna N, Mascolo R, et al. Polymer 2005;46:2105–21.
[8] Giamberini M, Amendola E, Carfagna C. Mol Cryst Liq Cryst 1995; 266:9–22.
[9] Williams G, Watts DC, Dev SB, North AM. Trans Faraday Soc 1971; 67:1323–35.
[10] Ortiz C, Ober CK, Kramer EJ. Polymer 1998;39:3713–8.
[11] Küpfer J, Finkelmann H. Makromol Chem Rapid Commun 1991;12: 717–26.
[12] De Vries A. Mol Cryst Liq Cryst 1985;131:125–45.
[13] Hotta A, Terentjev EM. J Phys Condens Matter 2001;13:11453–64.
[14] Clarke SM, Terentjev EM, Kundler I, Finkelmann H. Macromolecules 1998;31:4862–72.
[15] Schätzle J, Kaufhold W, Finkelmann H. Makromol Chem 1989;190: 3269–84.
[16] Ortiz C, Wagner M, Bhargava N, Ober CK, Kramer EJ. Macromolecules 1998;31:8531–9.
[17] Terentjev EM. J Phys Condens Matter 1999;11:R239–R57.
[18] Adams JM, Warner M. Eur Phys JE Soft Matter 2005;16:97–107.
[19] Terentjev EM, Warner M. Eur Phys JE Soft Matter 2001;4:343–53.
[20] Flory PJ. J Am Chem Soc 1945;67:2048–50.
[21] Yanko JA. J Polym Sci 1948;3:576–601.
[22] Nielsen LE, Landel RF. Mechanical properties of polymers and composites. 2nd ed. New York: Marcel Dekker; 1994. p. 255.
[23] Ferry J. Viscoelastic properties of polymers. New York: Wiley; 1980. p. 573 [and references therein].
[24] Mascolo R, Vestito C. PhD Thesis. University of Naples 'Federico II'; 2003.
[25] Nielsen LE, Landel RF. Mechanical properties of polymers and composites. 2nd ed. New York: Marcel Dekker; 1994 [chapter 3].
[26] Flory PJ. Principles of polymer chemistry. Ithaca, NY: Cornell University Press; 1953 [chapter 11].
[27] Aklonis JJ, Macknight WJ. Introduction to polymer viscoelasticity. 2nd ed. New York: Wiley; 1983 [chapter 6].
[28] Giamberini M, Amendola E, Carfagna C. Macromol Chem Phys 1997;198:3185–96.
[29] Anthony RL, Caston RH, Guth E. J Phys Chem 1942;46:826–40.
[30] Ferry J. Viscoelastic properties of polymers. New York: Wiley; 1980. p. 426.
[31] Zanna JJ, Stein P, Marty JD, Mauzac M, Martinoty P. Macromolecules 2002;35:5459–65.
[32] Weilepp J, Zanna JJ, Assfalg N, Stein P, Hilliou L, Mauzac M, et al. Macromolecules 1999;32:4566–74.
[33] Clarke SM, Tajbakhsh AR, Terentjev EM, Remillat C, Tomlinson GR, House JR. J Appl Phys 2001;89(11):6530–5.
[34] Stein P, Assfalg N, Finkelmann H, Martinoty P. Eur Phys JE 2001;4: 255–62.
[35] Terentjev EM, Warner M. Eur Phys JE 2001;4:343–53.
[36] Gallani JL, Hilliou P, Martinoty P, Doublet F, Mauzac M. J Phys II Fr 1996;6:443–52.
[37] Clarke SM, Hotta A, Tajbakhsh AR, Terentjev EM. Phys Rev E 2002; 65:021804.
[38] Hotta A, Terentjev EM. Eur Phys JE 2003;10:291–301.
[39] Martinoty P, Hilliou L, Mauzac M, Benguigui L, Collon D. Macromolecules 1999;32:1746–52.